

This is the accepted manuscript made available via CHORUS. The article has been published as:

Bounds on Majoron emission from muon to electron conversion experiments

Xavier Garcia i Tormo, Douglas Bryman, Andrzej Czarnecki, and Matthew Dowling

Phys. Rev. D **84**, 113010 — Published 20 December 2011

DOI: [10.1103/PhysRevD.84.113010](https://doi.org/10.1103/PhysRevD.84.113010)

Bounds on majoron emission from conversion experiments

Xavier Garcia i Tormo,^{1,*} Douglas Bryman,² Andrzej Czarnecki,¹ and Matthew Dowling¹

¹*Department of Physics, University of Alberta, Edmonton, Alberta, Canada T6G 2G7*

²*Department of Physics and Astronomy, University of British Columbia, Vancouver, British Columbia, Canada V6T 1Z1*

In models where lepton number is considered to be a spontaneously-broken global symmetry a massless Goldstone boson, the majoron (J), appears. We describe a procedure to explore the muon-electron-majoron coupling using the results from $\mu - e$ conversion search experiments. To accomplish that, we determine how the energy spectrum of the muon decay into an electron and a majoron is modified by binding effects in a muonic atom. We find that the future $\mu \rightarrow e$ conversion experiments may be able to produce bounds on the $\mu \rightarrow eJ$ rate which are comparable with the present ones from direct searches.

I. INTRODUCTION

The observation of neutrino oscillations has established that at least some of the neutrinos have mass [1]. The origin of the small neutrino mass differences and pattern of mixing angles which are seen in the experiments is not known at present. Exploring the nature of neutrino masses and mixing angles may allow us to glimpse particles and interactions beyond the Standard Model [2]. One class of models that generates neutrino masses, which could provide a possible explanation of the origin of the observed oscillations, considers lepton number as a spontaneously-broken global symmetry. In that case a massless Goldstone boson, the majoron (J) appears. Models of this kind were explored well before neutrino oscillations were experimentally established [3]. Some of those models [4, 5] predicted large additional contributions to the invisible decay width of the Z boson and were excluded after the Z -width measurement at LEP. It is possible, though, to construct supersymmetric models with spontaneous breaking of R -parity (and thus of lepton number) where no significant invisible Z -width is present, and the LEP bounds can be evaded [6].

In this paper, we focus on the model of Ref. [6] which permits charged-lepton decays with majoron emission [7]. Those processes were recently revisited in Ref. [8], where it was shown that the $\mu \rightarrow eJ$ decay rate is allowed to be large, and could potentially be in a region where it could be measured. It is quite interesting to study those decays, since they can explore regions of the supersymmetric parameter space that are not probed by collider searches. Experimentally it is quite a difficult task to improve on the current limits for the branching ratio $B(\mu \rightarrow eJ)$. In this paper we show that the future $\mu - e$ conversion experiments [9] may be able to produce bounds that are comparable to the present ones. Previous studies of (μ^-, e^+) conversion mechanisms involved majorons [10] in now disfavored models where the majoron is a gauge non-singlet.

The current limit for the branching ratio of a muon decaying to an electron and a majoron is [11]

$$B(\mu \rightarrow eJ) = \frac{\Gamma(\mu \rightarrow eJ)}{\Gamma(\mu \rightarrow e\nu_\mu\bar{\nu}_e)} < 8.4 \times 10^{-6}. \quad (1)$$

We will study $\mu - e$ conversion experiments, which can reach high sensitivities, and possibly improve on this limit. The $\mu - e$ conversion experiments produce muonic atoms (by stopping muons in a target) and then search for the process

$$\mu^- + (A, Z) \rightarrow e^- + (A, Z), \quad (2)$$

where (A, Z) represents a nucleus of atomic number Z and mass number A . The signal in conversion experiments is a mono-energetic electron at energy $E_{\mu e} = m_\mu - E_b - E_{rec}$ (with m_μ the muon mass, E_b the binding energy of the muonic atom, and E_{rec} the nuclear-recoil energy). If we now consider the process of $\mu \rightarrow eJ$ decay in the orbit of a nucleus (A, Z) , i.e.

$$\mu^- + (A, Z) \rightarrow e^- + J + (A, Z), \quad (3)$$

the outgoing electron can have energies up to the value of the conversion energy $E_{\mu e}$ since the nucleus can absorb momentum. $E_{\mu e}$ is also the maximum electron energy for muon decay in orbit (DIO), which constitutes the main

* Current address: Institut für Theoretische Physik, Universität Bern, Sidlerstrasse 5, CH-3012 Bern, Switzerland.

physics background source in the search for the conversion process in Eq. (2). Since the majoron J is not observed, the signal for the process in Eq. (3) would be electrons below $E_{\mu e}$. Therefore, the measurement of the electron spectrum close to $E_{\mu e}$, as is done in the conversion experiments, can be used to obtain a limit for $B(\mu \rightarrow eJ)$. The electron spectrum for the decay in Eq. (3) is a delta-function like shape around $E_e \sim m_\mu/2$ (where E_e is the electron energy) with a tail due to bound-state effects. The spectrum for the two-body free decay $\mu \rightarrow eJ$ is just a delta function at $E_e \sim m_\mu/2$. Even though we only look for events at the high-energy tail of the electron-energy spectrum in $\mu \rightarrow eJ$ decay in orbit, the fact that the current limit in Eq. (1) is not very stringent, combined with the high sensitivity that the future conversion experiments are expected to reach, might allow them to improve on the present constraints. The $\mu \rightarrow e$ conversion experiments provide a limit on $B(\mu \rightarrow eJ)$ by first determining

$$\frac{\Gamma(\mu(A, Z) \rightarrow e(A, Z))}{\Gamma_{\text{capture}}} =: R_{\mu e}, \quad (4)$$

where Γ_{capture} is the rate of the nuclear muon capture, $\Gamma_{\text{capture}} = \Gamma(\mu + (A, Z) \rightarrow (A, Z-1) + \nu_\mu)$. This result places a bound on the majoron emission in muon decay according to

$$\frac{\Gamma(\mu \rightarrow eJ) \times f_J}{\Gamma_{\text{capture}}} \sim N_R R_{\mu e}, \quad (5)$$

where f_J is the fraction of $\mu \rightarrow eJ$ decay in orbit events in the signal region of the conversion experiment and N_R is a correction factor for the phase space region used in the search for $\mu + (A, Z) \rightarrow e + J + (A, Z)$. The limit on the branching ratio is then given by

$$B(\mu \rightarrow eJ) = \frac{\Gamma(\mu \rightarrow eJ)}{\Gamma(\mu \rightarrow e\nu_\mu\bar{\nu}_e)} \sim \frac{N_R R_{\mu e}}{f_J} \frac{\Gamma_{\text{capture}}}{\Gamma(\mu \rightarrow e\nu_\mu\bar{\nu}_e)}. \quad (6)$$

In the near future, the DeeMe Collaboration [12] has proposed to reach $R_{\mu e} \sim 10^{-14}$ sensitivity. Furthermore, the planned conversion experiments, Mu2e at Fermilab [13] and COMET at J-PARC [14], aim for sensitivities at the $R_{\mu e} \sim 10^{-16}$ level; in addition, both experiments are speculating on a later phase which would aim for a sensitivity of 10^{-18} . Comparing Eq. (6) with the present limit in Eq. (1) we can examine the potential of those experiments to improve on the present bounds, as long as the factor $(f_J \Gamma(\mu \rightarrow e\nu_\mu\bar{\nu}_e))/(\Gamma_{\text{capture}} N_R)$ is not much smaller than 10^{-11} .

The paper is organized as follows: in Sec. II we compute the electron spectrum for the $\mu \rightarrow eJ$ decay in atomic orbit. Then in Sec. III, we present our numerical results and discuss in detail the bounds that we can obtain for the branching ratio $B(\mu \rightarrow eJ)$. We conclude in Sec. IV.

II. MAJORON EMISSION IN ORBIT

Our aim is to calculate the electron spectrum for majoron emission $\mu \rightarrow eJ$ in orbit (MEIO), i.e. the process in Eq. (3).

We write the interaction that mediates majoron emission in muon decay $\mu \rightarrow eJ$ as

$$\mathcal{L} = \bar{\mu} g_1 P_R e J + \bar{\mu} g_2 P_L e J, \quad (7)$$

where $P_R = (1 + \gamma_5)/2$ and $P_L = (1 - \gamma_5)/2$. The couplings g_1 and g_2 are dimensionless, i.e. they can be written in terms of parameters of the underlying supersymmetric model [8]. The matrix element for the free $\mu \rightarrow eJ$ decay is given by

$$\mathcal{M} = \bar{u}(p_e) (g_1 P_R + g_2 P_L) u(p_\mu) \quad ; \quad |\mathcal{M}|^2 = \bar{u}(p_e) (g_1 P_R + g_2 P_L) u(p_\mu) \bar{u}(p_\mu) (g_1 P_L + g_2 P_R) u(p_e), \quad (8)$$

where p_μ and p_e are the momentum of the muon and the electron, respectively. Summing over the electron spin and averaging over the muon spin we obtain

$$\overline{\sum} |\mathcal{M}|^2 = (g_1^2 + g_2^2) p_e \cdot p_\mu, \quad (9)$$

where we considered the electron to be massless. We always consider a massless electron in this paper, since we are interested in the high-energy part of the spectrum for MEIO. The free decay rate, Γ_0 , is then given by

$$\Gamma_0 = \frac{1}{2m_\mu} \int \frac{d^3 p_e}{(2\pi)^3 2E_e} \frac{d^3 p_J}{(2\pi)^3 2E_J} (2\pi)^4 \delta^{(4)}(p_\mu - p_e - p_J) \overline{\sum} |\mathcal{M}|^2$$

$$= \frac{g_1^2 + g_2^2}{16\pi} \int dE_e \frac{E_e^2}{m_\mu - E_e} \delta\left(E_e - \frac{m_\mu}{2}\right) = \frac{(g_1^2 + g_2^2)m_\mu}{32\pi}, \quad (10)$$

where $p_J = (E_J, \vec{p}_J)$ is the majoron 4-momentum. Obviously, since this is a 2-body decay, the electron-energy spectrum is just a δ function at $E_e = m_\mu/2$. For MEIO Eq. (10) gets replaced by

$$\Gamma = \sum_{e^- \text{ spin}} \int \frac{d^3 p_e}{(2\pi)^3 2E_e^2} \frac{d^3 p_J}{(2\pi)^3 2E_J} (2\pi) \delta(E_\mu - E_e - E_J) \mathcal{J} \mathcal{J}^\dagger, \quad (11)$$

where $E_\mu = m_\mu - E_b$, and

$$\mathcal{J} := \int d^3 r e^{-i\vec{p}_J \cdot \vec{r}} \bar{\varphi}_e (g_1 P_R + g_2 P_L) \varphi_\mu, \quad (12)$$

where φ_e and φ_μ are the solutions of the Dirac equation (in the potential created by the nucleus) for the electron and the muon, respectively. We incorporate the average over the muon spin in the definition of φ_μ , while we do not incorporate the sum over the electron spin in the definition of φ_e . When the muonic atom is formed the muon cascades down almost immediately to the ground state, and this process also depolarizes the muon [15]. We consider an unpolarized muon in the $1S$ state and write the muon wavefunction as

$$\varphi_\mu(\vec{r}) = \sum_s a_s \begin{pmatrix} G\chi_{-1}^s \\ iF\chi_1^s \end{pmatrix}, \quad (13)$$

where a_s is the amplitude of the muon state with spin projection s . For an unpolarized muon we have $|a_s|^2 = 1/2$. $\chi_\kappa^\mu = \chi_\kappa^\mu(\hat{r})$ are the spin-angular functions, which are given by

$$\chi_\kappa^\mu = \sum_m C\left(l\frac{1}{2}j; \mu - m \ m \ \mu\right) Y_l^{\mu-m} \chi^m, \quad (14)$$

with $C(ls j; l_z s_z j_z)$ the Clebsch-Gordan coefficients, Y_l^μ are the spherical harmonics and χ^m are the spin 1/2 eigenfunctions. G and F are the solutions of the radial Dirac equations, which are taken to be normalized as

$$\int r^2 (F^2 + G^2) dr = 1. \quad (15)$$

The electron wavefunction is expanded in partial waves according to

$$\varphi_e(\vec{r}) = \sum_{\kappa\mu} a_{\kappa\mu t} \psi_\kappa^\mu = \sum_{\kappa\mu} a_{\kappa\mu t} \begin{pmatrix} g_\kappa \chi_\kappa^\mu \\ i f_\kappa \chi_{-\kappa}^\mu \end{pmatrix}, \quad (16)$$

where g_κ and f_κ are the solutions of the radial Dirac equations for the electron, labeled by $\kappa = \pm 1, \pm 2, \dots$ [16], t is the z -component of the electron spin, and the $a_{\kappa\mu t}$ coefficients are given by

$$a_{\kappa\mu t} = i^{l_\kappa} \frac{4\pi}{\sqrt{2}} C\left(l_\kappa \frac{1}{2} j_\kappa; \mu - t \ t \ \mu\right) Y_{l_\kappa}^{\mu-t*}(\hat{p}_e) e^{-i\delta_\kappa}, \quad (17)$$

where δ_κ is the Coulomb phase shift (the distortion from a plane wave due to the potential of the nucleus), $j_\kappa = |\kappa| - 1/2$, and $l_\kappa = j_\kappa - \text{Sign}(\kappa)/2$. The electron wavefunctions are normalized in the energy scale, according to

$$\int d^3 r \psi_{\kappa,W}^{\mu*} \psi_{\kappa',W'}^{\mu'} = 2\pi \delta_{\mu\mu'} \delta_{\kappa\kappa'} \delta(W - W'), \quad (18)$$

where $\psi_{\kappa,W}^\mu$ corresponds to a solution with energy W .

We ignored nuclear-recoil effects to write Eq. (11) but will incorporate them later. Integrating over the solid angle in Eq. (12) we obtain

$$\begin{aligned} \mathcal{J} &= \frac{\sqrt{4\pi}}{2} \sum_{KM} (-i)^K \sum_{s\kappa\mu} a_{\kappa\mu t}^* a_s \int dr r^2 j_K(p_J r) C\left(K \frac{1}{2} j_\kappa; M s \mu\right) Y_K^{M*}(\hat{p}_J) \\ &\times \left\{ (g_1 + g_2) (g_\kappa G - f_\kappa F) \delta_{Kl_\kappa} + i(g_1 - g_2) (f_\kappa G + g_\kappa F) \delta_{Kl_{-\kappa}} \right\}. \end{aligned} \quad (19)$$

We can then write the result for the spectrum,

$$\frac{1}{\Gamma_0} \frac{d\Gamma}{dE_e} = \sum_{K\kappa} \frac{1}{\pi m_\mu} (2j_\kappa + 1) [E_\mu - E_e] |\mathcal{S}_{K\kappa}|^2, \quad (20)$$

where

$$\mathcal{S}_{K\kappa} := \int dr r^2 j_K ([E_\mu - E_e] r) \{ (g_\kappa G - f_\kappa F) \delta_{Kl_\kappa} + i (f_\kappa G + g_\kappa F) \delta_{Kl_{-\kappa}} \}. \quad (21)$$

In Eq. (20), the sum over K goes from 0 to ∞ , and for a given value of K , κ can only take the values $\pm K$ and $\pm(K+1)$, but κ can never be equal to 0. $j_n(z)$ is the spherical Bessel function of order n .

Since future $\mu \rightarrow e$ conversion experiments may use aluminum or heavier nuclei as targets, the nucleus is, at least, more than 200 times heavier than the muon and nuclear-recoil effects are negligible for most of the electron spectrum. Recoil effects could be important close to the high-energy endpoint since they modify the maximum allowed electron energy. In that region we can approximate the nuclear-recoil energy E_{rec} as [17]

$$E_{\text{rec}} = \frac{|\vec{p}_N|^2}{2m_N} \simeq \frac{E_e^2}{2m_N}, \quad (22)$$

with m_N the mass of the nucleus and \vec{p}_N its three-momentum. Within this approximation, the inclusion of recoil effects reduces to the substitution

$$E_\mu - E_e \rightarrow E_\mu - E_e - \frac{E_e^2}{2m_N}, \quad (23)$$

inside the square brackets in Eqs. (20) and (21). The endpoint is now at $E_e = E_\mu - E_\mu^2/(2m_N)$. Inclusion of nuclear-recoil effects beyond the approximation in the equations above is unnecessary for all practical purposes. Our final result for the electron spectrum in MEIO then reads

$$\frac{1}{\Gamma_0} \frac{d\Gamma}{dE_e} = \sum_{K\kappa} \frac{1}{\pi m_\mu} (2j_\kappa + 1) \left[E_\mu - E_e - \frac{E_e^2}{2m_N} \right] |\mathcal{S}_{K\kappa}|^2, \quad (24)$$

with

$$\mathcal{S}_{K\kappa} := \int dr r^2 j_K \left(\left[E_\mu - E_e - \frac{E_e^2}{2m_N} \right] r \right) \{ (g_\kappa G - f_\kappa F) \delta_{Kl_\kappa} + i (f_\kappa G + g_\kappa F) \delta_{Kl_{-\kappa}} \}. \quad (25)$$

A. Taylor expansion around the endpoint

We can perform a Taylor expansion of the electron energy spectrum in Eq. (24) around the endpoint to make its behavior manifest. For that, we need the Taylor expansion of $\mathcal{S}_{K\kappa}$ in Eq. (25). We obtain, noting that the electron wavefunctions g_κ and f_κ depend on E_e ,

$$\begin{aligned} \mathcal{S}_{K\kappa} = & \int dr r^2 (g_{-1}G - f_{-1}F) \delta_{0K} \delta_{-1\kappa} \\ & + \int dr r^2 \left\{ \frac{r}{3} \left(1 + \frac{E_\mu}{m_N} \right) [i (f_{-1}G + g_{-1}F) \delta_{1K} \delta_{-1\kappa} + (g_{-2}G - f_{-2}F) \delta_{1K} \delta_{-2\kappa}] \right. \\ & \left. - (g'_{-1}G - f'_{-1}F) \delta_{0K} \delta_{-1\kappa} \right\} \left(E_\mu - E_e - \frac{E_e^2}{2m_N} \right) + \mathcal{O} \left(\left(E_\mu - E_e - \frac{E_e^2}{2m_N} \right)^2 \right), \end{aligned} \quad (26)$$

where

$$f'_\kappa := \frac{df_\kappa}{dE_e} \quad ; \quad g'_\kappa := \frac{dg_\kappa}{dE_e}. \quad (27)$$

It is understood that the electron wavefunctions in Eq. (26) (or their derivatives) are evaluated at the endpoint energy $E_e = E_\mu - E_\mu^2/(2m_N)$. The corresponding Taylor expansion without including recoil effects is recovered by taking the limit $m_N \rightarrow \infty$. Since we have the property

$$\int dr r^2 g_{-1}G = \int dr r^2 f_{-1}F, \quad (28)$$

TABLE I. Values for the parameters in the Fermi distribution in Eq. (29) [18], nuclear masses, muon energy E_μ , and endpoint energy $E_{\mu e}$, for the elements used in the text.

| Nucleus | r_0 (fm) | a (fm) | m_N (MeV) | E_μ (MeV) | $E_{\mu e}$ (MeV) |
|----------------|------------|----------|-------------|---------------|-------------------|
| Al($Z = 13$) | 2.84 | 0.569 | 25133 | 105.194 | 104.973 |
| Ti($Z = 22$) | 3.84 | 0.588 | 44588 | 104.394 | 104.272 |
| Au($Z = 79$) | 6.38 | 0.535 | 183473 | 95.533 | 95.508 |

when the energies of the muon and the electron are equal [17], the leading term in the expansion of $\mathcal{S}_{K\kappa}$ vanishes when we neglect nuclear-recoil effects. Therefore, the Taylor expansion of the electron spectrum without nuclear-recoil effects starts at order $(E_\mu - E_e)^3$. If we take nuclear recoil into account the leading term of the Taylor expansion for $\mathcal{S}_{K\kappa}$ no longer vanishes exactly, but it is suppressed by the inverse of m_N .

III. BOUNDS ON THE BRANCHING RATIO

Equation (24) gives the electron spectrum for MEIO. We will use it here to obtain bounds for the branching ratio $B(\mu \rightarrow eJ)$. We solve the Dirac equation numerically to obtain the electron (g_κ and f_κ) and muon (G and F) wavefunctions that appear in Eq. (24). To do that, we consider a nucleus of finite size, characterized by a two-parameter Fermi distribution $\rho(r)$, given by

$$\rho(r) = \rho_0 \frac{1}{1 + e^{\frac{r-r_0}{a}}}. \quad (29)$$

The parameters r_0 and a , the nuclear masses, the muon binding energy E_μ , and the endpoint energy $E_{\mu e}$ for the elements of current experimental interest are summarized in Table I. The normalization factor ρ_0 in Eq. (29) is determined from the condition $\int d^3r \rho(r) = -Z\alpha$. For the muon mass and the fine structure constant we use the values $m_\mu = 105.6584$ MeV, $\alpha = \frac{1}{137.036}$. Radiative corrections were not included in Eq. (24) but are not expected to significantly modify the results. Note that, as it happens for the usual muon DIO (see Ref. [19]), to obtain the correct result for the high-energy tail of the spectrum it is necessary to include finite nuclear size effects, the interaction of the outgoing electron with the field of the nucleus, the Dirac (rather than Schrödinger) wavefunction for the muon and (at least for not very heavy elements) nuclear-recoil effects, as we did.

Conversion experiments measure the electron spectrum in a window of a few MeV near the energy $E_{\mu e}$, in search for a peak that would reveal the conversion process in Eq. (2). In this energy window, electrons from muon DIO are also present and are seen by the experiments. The spectrum for muon DIO has been recently studied in detail [19] and it is now under good theoretical control. Electrons coming from MEIO would appear as an additional contribution on top of the electrons coming from muon DIO.

A. Existing conversion results

Currently the most stringent upper limit for the conversion branching ratio is given by the SINDRUM II Collaboration, $R_{\mu e} < 7 \times 10^{-13}$ (90% C.L.), using a gold (Au, $Z = 79$) target [20]. Ref. [20] measured the electron spectrum in a region from 90 MeV to $E_{\mu e}$. From Eq. (24) we obtain the electron spectrum for MEIO for gold, which for illustration we plot in Fig. 1 as the solid line. We find that the MEIO spectrum for energies $E_e > 90$ MeV is very well fitted by

$$\frac{1}{\Gamma_0} \frac{d\Gamma}{dE_e} \Big|_{\text{Au, } E_e > 90 \text{ MeV}} = \frac{1}{m_\mu} (5.292 \times 10^{-3} \delta^3 + 9.629 \times 10^{-2} \delta^4 + 1.125 \delta^5 + 22.94 \delta^6), \quad (30)$$

where

$$\delta := \frac{E_\mu - E_e - \frac{E_e^2}{2m_N}}{m_\mu}. \quad (31)$$

Since the gold nucleus is quite heavy, the terms proportional to δ and δ^2 in the spectrum are found to be negligibly small (see the discussion in Sec. II A). The fraction f_J of $\mu \rightarrow eJ$ decay in orbit events for energies above 90 MeV is

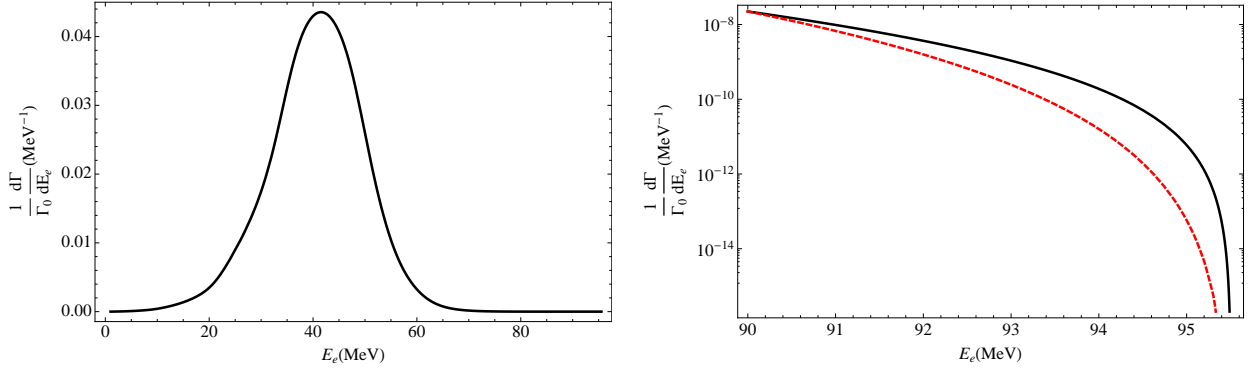


FIG. 1. Electron spectrum for majoron emission in orbit for gold (solid line). The second panel is a zoom for $E_e > 90$ MeV. The dashed line in the second panel is the electron spectrum for DIO in gold, multiplied by a constant ($C = 333$) to make it coincide with the MEIO rate at $E_e = 90$ MeV.

given by

$$f_J|_{Au, E_e > 90 \text{ MeV}} = \int_{90 \text{ MeV}}^{E_{\mu e}} \frac{1}{\Gamma_0} \frac{d\Gamma}{dE_e} dE_e = 2.4 \times 10^{-8}. \quad (32)$$

The total muon lifetime in gold is 88 ns, determined by the capture rate. Therefore, using the estimate for the limit on the branching ratio that we derived in Eq. (6), we have

$$B(\mu \rightarrow eJ) \sim \frac{N_R R_{\mu e}}{f_J} \frac{\Gamma_{\text{capture}}}{\Gamma(\mu \rightarrow e\nu_\mu \bar{\nu}_e)} \sim \frac{N_R R_{\mu e}}{f_J} \frac{2.197 \mu s}{88 \text{ ns}} \sim \frac{N_R R_{\mu e}}{f_J} 25, \quad (33)$$

where we also used that the free muon width is $\Gamma(\mu \rightarrow e\nu_\mu \bar{\nu}_e) = 1/(2.197 \mu s)$, and N_R is the factor representing the event distribution observed below the conversion peak. The upper limit $R_{\mu e} < 7 \times 10^{-13}$ set by Ref. [20] was obtained from a likelihood analysis considering the mono-energetic conversion signal, muon DIO, and additional backgrounds from radiative muon capture, pion decays and cosmic rays. The shape of the electron energy distribution seen in the experiment was well described by muon DIO. It is reasonable to assume that the events seen in the region $E_e > 90$ MeV came from muon DIO and that no additional events from majoron emission were present. Nevertheless, to avoid doing background subtractions of DIO events, we will consider that the number of MEIO events cannot be larger than those seen in the experiment. Six events were seen for $E_e > 90$ MeV, and if we assume a Gaussian distribution (with mean and variance equal to 6), the 90% C.L. limit corresponds to 9 events. Therefore, to obtain the limit on $B(\mu \rightarrow eJ)$, we use Eq. (33) with the factor $N_R = 9/2.3$ (where the 2.3 in the denominator corresponds to the events for 90% C.L. on a Poisson distribution with expected number of occurrences 1 or 0). Doing that we obtain

$$B(\mu \rightarrow eJ) \lesssim \frac{N_R R_{\mu e}}{f_J} 25 \sim \frac{\frac{9}{2.3} 7 \times 10^{-13}}{2.4 \times 10^{-8}} 25 \sim 3 \times 10^{-3}. \quad (34)$$

The upper limit in Eq. (34) is still less restrictive than the current limit in Eq. (1). Thus, the existing conversion data does not improve on the present limits for the $\mu - e - J$ coupling.

B. New conversion experiments (Mu2e and COMET)

Future $\mu \rightarrow e$ conversion experiments Mu2e at Fermilab [13] and COMET at J-PARC [14] aim to reach sensitivities at the 10^{-16} level, and to use an aluminum (Al, $Z = 13$) target. The ratio of muon capture width in Al over the free muon width is around 1.5 (as compared to 25 for Au, as in Eq. (33)), but f_J is lower due to the much lower Z . The $\mu \rightarrow e$ conversion energy in Al is around 105 MeV (see Table I). Using $E_e > 100$ MeV as the signal region, f_J for Al is 2.2×10^{-10} , and $N_R = 27$ based on subtraction of the DIO background, resulting in

$$B(\mu \rightarrow eJ) \sim \frac{N_R R_{\mu e}}{f_J} \frac{\Gamma_{\text{capture}}}{\Gamma(\mu \rightarrow e\nu_\mu \bar{\nu}_e)} \sim \frac{N_R R_{\mu e}}{f_J} 1.5 \sim \frac{27 \times 10^{-16}}{2.2 \times 10^{-10}} 1.5 \sim 1.9 \times 10^{-5}, \quad (35)$$

which is comparable to the current limit in Eq. (1). If a sensitivity of 10^{-18} is reached, the limit on $B(\mu \rightarrow eJ)$ will improve by an order of magnitude due to improved statistical precision on DIO.

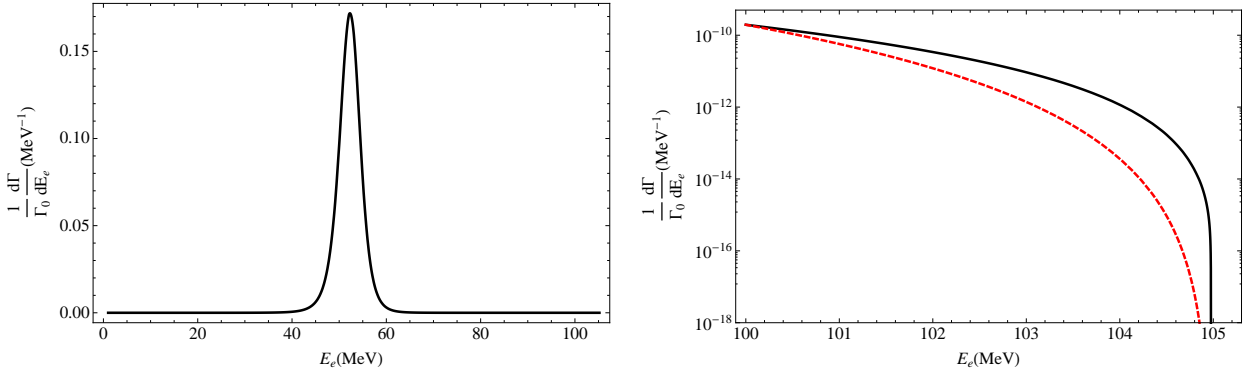


FIG. 2. Electron spectrum for majoron emission in orbit for Al (solid line). The second panel is a zoom for $E_e > 100$ MeV. The dashed line in the second panel is the electron spectrum for DIO in Al, multiplied by a constant ($C = 415$) to make it coincide with the MEIO rate at $E_e = 100$ MeV.

To obtain a more detailed estimate of the upper limit for $B(\mu \rightarrow eJ)$ that Mu2e and COMET could obtain, we need to convolute the MEIO spectrum with the experimental energy resolution modeled by those collaborations. Once again, from Eq. (24) we get the electron spectrum for MEIO for Al, which for illustration we plot in Fig. 2 as the solid line. We find that the spectrum for energies $E_e > 100$ MeV is very well fitted by¹

$$\left. \frac{1}{\Gamma_0} \frac{d\Gamma}{dE_e} \right|_{Al, E_e > 100 \text{ MeV}} = \frac{1}{m_\mu} (3.289 \times 10^{-10} \delta + 3.137 \times 10^{-7} \delta^2 + 1.027 \times 10^{-4} \delta^3 + 1.438 \times 10^{-3} \delta^4 + 2.419 \times 10^{-3} \delta^5 + 1.215 \times 10^{-1} \delta^6). \quad (36)$$

Convoluting the above equation with the estimated energy resolution of the experiment (which we denote as $F(E_e)$) we can obtain a value of f_J

$$f_J|_{E_e > x} = \int_x^{E_{\mu e}} \left(\frac{1}{\Gamma_0} \frac{d\Gamma}{dE_e} \otimes F \right) dE_e, \quad (37)$$

where \otimes denotes the convolution. Using the estimated energy resolution for Mu2e and COMET, and estimating the expected number of DIO events in the signal region ($N_{\text{DIO}} \simeq 2400$), we find that the bound on $B(\mu \rightarrow eJ)$ that a conversion experiment with $R_{\mu e} \sim 10^{-16}$ on Al may be able to place will be $B(\mu \rightarrow eJ) < 2 \times 10^{-5}$, roughly at the same level as the current one in Eq. (1).

Since COMET and Mu2e also consider Ti as a viable target we give, for completeness, the polynomial that fits the MEIO spectrum in Ti for $E_e > 99$ MeV²

$$\left. \frac{1}{\Gamma_0} \frac{d\Gamma}{dE_e} \right|_{Ti, E_e > 99 \text{ MeV}} = \frac{1}{m_\mu} (5.404 \times 10^{-10} \delta + 9.301 \times 10^{-7} \delta^2 + 5.552 \times 10^{-4} \delta^3 + 8.113 \times 10^{-3} \delta^4 + 5.470 \times 10^{-2} \delta^5 + 4.244 \times 10^{-1} \delta^6). \quad (38)$$

The bounds on $B(\mu \rightarrow eJ)$ we would obtain with a Ti target are similar to those for Al.

C. Discussion

We have shown in the previous section that a $\mu \rightarrow e$ conversion experiment with an Al target and sensitivity at the $10^{-16} - 10^{-18}$ level may be able to produce bounds on the $\mu - e - J$ coupling which are competitive with the

¹ Eq. (36) may be used in a wider energy range. It reproduces Eq. (24) for Al with an accuracy better than 10% until $E_e \sim 90$ MeV.

² It can be used until $E_e \sim 93$ MeV to reproduce Eq. (24) for Ti with an accuracy better than 10%.

present ones. If the electron distribution seen in the experiments around $E_{\mu e}$ agrees well with DIO, the procedure we have presented allows to place a bound on $B(\mu \rightarrow eJ)$. If it is found that the electron distribution is not well described by DIO, it could be checked if the addition of a component following Eq. (36) improves the agreement which could be consistent with the presence of events coming from MEIO. Note that (when we neglect nuclear-recoil effects) the electron spectrum for MEIO goes as $\sim (E_{\mu e} - E_e)^3$ near the endpoint, while the usual muon DIO goes as $\sim (E_{\mu e} - E_e)^5$. MEIO is, therefore, less suppressed than DIO in this region, and the endpoint is a favorable region to search for the $\mu \rightarrow eJ$ process. To compare the shapes of the two processes near the endpoint, we also show in the second plot in Fig. 2 (Fig. 1) the electron spectrum for DIO in Al (Au) as the dashed line [19], multiplied by a constant $C = 415$ ($C = 333$) to make it coincide with the MEIO value at $E_e = 100$ MeV ($E_e = 90$ MeV).

One may also ask which target materials give better sensitivity to $B(\mu \rightarrow eJ)$. When we increase Z , the fraction f_J increases (which improves the bound one would obtain), but the capture width and N_R also increase (which worsens the bound one would obtain). The net result is that, for a given sensitivity to the conversion search, the sensitivity to $B(\mu \rightarrow eJ)$ is roughly independent of Z .

IV. CONCLUSIONS

We have computed the electron spectrum for the $\mu \rightarrow eJ$ decay when the muon is orbiting a nucleus. Using those results, we described a procedure to probe the muon-electron-majoron coupling using $\mu \rightarrow e$ conversion experiments. Using results of conversion experiments to improve the limit on $B(\mu \rightarrow eJ)$ does not require any dedicated experimental search. $B(\mu \rightarrow eJ)$ can also be probed in $\mu \rightarrow e\gamma$ searches [8], although some relaxation in the cuts of those experiments is required to improve the present limits. The future conversion experiments, Mu2e and COMET, may have the capability to produce bounds on $B(\mu \rightarrow eJ)$ that are competitive with the present ones, and possibly improve them. The results presented in this paper strengthen the physics case for the upcoming conversion experiments.

ACKNOWLEDGMENTS

This research was supported by the Science and Engineering Research Canada (NSERC). AC thanks the Institute for Nuclear Theory at the University of Washington for its hospitality and the US Department of Energy for partial support during the completion of this work.

-
- [1] T. Schwetz, M. Tortola and J. W. F. Valle, New J. Phys. **13**, 063004 (2011) [arXiv:1103.0734 [hep-ph]]. T. Schwetz, M. Tortola, J. W. F. Valle, New J. Phys. **13**, 109401 (2011). [arXiv:1108.1376 [hep-ph]].
 - [2] M. C. Gonzalez-Garcia, M. Maltoni, Phys. Rept. **460**, 1-129 (2008). [arXiv:0704.1800 [hep-ph]].
 - [3] Y. Chikashige, R. N. Mohapatra, R. D. Peccei, Phys. Lett. **B98**, 265 (1981).
 - [4] G. B. Gelmini, M. Roncadelli, Phys. Lett. **B99**, 411 (1981).
 - [5] C. S. Aulakh, R. N. Mohapatra, Phys. Lett. **B119**, 136 (1982).
 - [6] A. Masiero, J. W. F. Valle, Phys. Lett. **B251**, 273-278 (1990).
 - [7] J. C. Romao, N. Rius, J. W. F. Valle, Nucl. Phys. **B363**, 369-384 (1991).
 - [8] M. Hirsch, A. Vicente, J. Meyer, W. Porod, Phys. Rev. **D79**, 055023 (2009). [arXiv:0902.0525 [hep-ph]].
 - [9] Y. Kuno, in B. L. Roberts and W. J. Marciano (eds.), "Lepton Dipole Moments", World Scientific (Singapore, 2009) (Adv. Ser. Dir. HEP 20), p. 701.
 - [10] M. S. Zahir and C. E. Picciotto, Nucl. Phys. **B219**, 23 (1983).
 - [11] R. Bayes, Ph.D. thesis (University of Victoria, 2010).
 - [12] M. Aoki, PoS **ICHEP 2010**, 279 (2010).
 - [13] R. M. Carey *et al.* [Mu2e Collaboration], "Proposal to search for $\mu^- N \rightarrow e^- N$ with a single event sensitivity below 10^{-16} ", Fermilab Proposal 0973 (2008).
 - [14] Y. G. Cui *et al.* [COMET Collaboration], "Conceptual design report for experimental search for lepton flavor violating $\mu^- - e^-$ conversion at sensitivity of 10^{-16} with a slow-extracted bunched proton beam (COMET)", KEK Report 2009-10.
 - [15] A. Grossheim *et al.* [TWIST Collaboration], Phys. Rev. **D80**, 052012 (2009) [arXiv:0908.4270].
 - [16] M. E. Rose, "Relativistic Electron Theory", Wiley, New York, 1961.
 - [17] O. U. Shanker, Phys. Rev. **D25**, 1847 (1982).
 - [18] H. De Vries, C. W. De Jager, and C. De Vries, Atom. Data Nucl. Data Tabl. **36**, 495-536 (1987).
 - [19] A. Czarnecki, X. Garcia i Tormo, W. J. Marciano, Phys. Rev. **D84**, 013006 (2011). [arXiv:1106.4756 [hep-ph]].
 - [20] W. H. Bertl *et al.* [SINDRUM II Collaboration], Eur. Phys. J. **C47**, 337 (2006).